413
GEOME 2
Manuscript received: September 19, 2024
Accepted: November 15, 2024

Geologica Macedonica, Vol**. 38**, No. 2, pp. 105–114 (2024)
On print ISSN 0352 – 1206
On line ISSN 1857 – 8586
UDC: 550.348.098.33:[691.3.04:534.1(497.735)
https://doi.org/10.46763/GEOL24382105k

Original scientific paper

ANALYSIS OF MICROTREMORS BY MEASURING AND PROCESSING OF AMBIENT VIBRATIONS TESTS

Mirjana Kocaleva Vitanova, Vlado Gičev

Faculty of Computer Science, Goce Delcev University,
Krste Misirkov 10A, Stip, Republic of North Macedonia
mirjana.kocaleva@ugd.edu.mk

A b s t r a c t: Microtremors, small-scale ground vibrations typically with amplitudes ranging from micrometers to millimeters, have emerged as a valuable tool for studying various aspects of Earth's subsurface properties and dynamics. This paper provides an overview of the methodologies employed in the detection, analysis, and interpretation of microtremors for a two-story reinforced concrete building located in Berovo.

Key words: natural disasters; microtremors; peak-to-peak amplitudes

INTRODUCTION

Mother Nature is one of the most complicated and powerful systems on planet Earth. We live in a world where we constantly face natural disasters such as earthquakes, floods, tsunamis, volcano eruptions, and other geological processes. These disasters, in addition to causing material damage, are sometimes fatal to people's lives. That's why measurements are made every day, a variety of research is done, all with the same goal – to be prepared for disasters and their consequences, as well as to find a way to protect ourselves from them. The goal of earthquake engineering is to design earthquake-resistant buildings, and the beginning of modern earthquake engineering was laid by Maurice Biot in 1932 with his spectral response method.

Our attention is devoted to the disasters caused by earthquakes. An earthquake is a shaking of the earth. Every year there are many earthquakes, caused by a variety of factors, including people's activities. Nowadays, the instruments measuring strong ground motions are sensitive enough that apart from earthquakes, they can also register microvibrations of buildings during everyday events, such as traffic around the building, wind, movement of people in the building, etc. These stimuli are called ambient stimuli, and the objects' response to them, ambient vibrations.

In the beginning, ambient vibrations tests were used for obtaining fundamental periods of buildings (Carder, 1936). After thirty years, the interest in the method revived. Since 1970's the ambient tests were conducted in many buildings (Trifunac, 1970, 1971; Trifunac et al., 1999, 2001; Moslem and Trifunac 1986; Mulhern & Maley, 1973; Luco et al., 1975; Wong et al., 1977). Nowadays, the ambient vibration tests continue to be used mostly for obtaining the natural frequencies and mode shapes of various full-scale structures (Ko & Bao, 1985; Rodriguez-Cuevas, 1989; Taskov and Krstevska, 1998), bridges (Abdel-Ghaffar et al., 1984; Abdel-Ghaffar & Housner, 1977, 1978; Brownjohn, 2003, 2007), dams (Abdel-Ghaffar & Scott, 1981), industrial chimneys (Kapsarov & Milicevic, 1986), and nuclear power plants (Klasky et al., 1973; Luz et al., 1983).

DESCRIPTION OF THE OBJECT AND THE INSTRUMENT

The facility we are analyzing and measuring a house located in Berovo, near the northern shore of Lake Berovo, 940 meters above sea level (Figure 1). The house is a two-story reinforced concrete building with a partially buried basement and attic. Two measurements were carried out in the house. The

first measurement was performed at 2 points, one at the basement and one at the top, to calibrate the instruments and the second measurement was carried out at 68 different points all over the house (Gicev, 2021; Kokalanov, 2022).

a)

b)

Fig. 1. Weekend house at Berovo Lake: a) north-east view, b) south-west view

In this research we work with data obtained using field measurements using two EQResponder120 accelerometers. EQR120 accelerometers are highly sensitive and therefore able to register ambient noise (CS Instruments, 2019). First, the accelerometers were synchronized by GPS antennas using an internet connection. GPS antennas need to be placed under the open sky and receive a good satellite signal to synchronize the time of both instruments. At the same time, by placing the instruments near the ends of the roof and recording the ambient vibrations in the direction of the length and width of the building, the torsional periods of the measured buildings can be determined (Rahmani & Todorovska, 2014; Sawada, 2004). The accelerometers are normally set to continuous operation and each one should be synchronized to UTC (Coordinated Universal Time) from its own GPS receivers (accuracy 1 μs). Each EQR120 is a triaxial accelerometer with a MEMS servo silicon sensor with a dynamic range of 128 dB (0.1 – 20 Hz) and a recording range of ±4 g, with implications of a recording threshold level of 2.4×10^{-6}g (g = $9.81\ \mathrm{m/s^2}$= acceleration due to gravity) or 2.4×10^{-3}gal. They have offset error < ± 0.02%, linearity error < ± 0.1%, and gain error < ± 0.08%, over the operating temperature range (–10 to +60 °C).

In the mode of measuring strong ground motions, to study the structural response using two instruments only, the accelerometers are usually placed one in the basement (we call it Slave) and the other on the top floor, in the attic (we call it Master). In this mode, the instruments do not measure until some external excitation above previously set threshold, triggers them to register accelerations. The measurement is stopped when the ratio of the short-term and long-term mean value of the acceleration STA/LTA is lower than a previously set threshold. When we measure ambient vibrations, the measurement mode is continuous and the accelerometers record data in files, which are closed every 10 minutes, 30 minutes, 1 hour, 2 hours or 6 hours depending on how it is selected in the settings. If the sensors are set to continuous operation mode, we need to wait for the file to close and reset the sensor. Data is never lost.

METHODOLOGY

To process the data accordingly, we worked according to the following concept: With the instruments, we measured accelerations at different points in the house generated by environmental stimuli (traffic, wind, movements in objects, etc.) over time. We measure in three directions: *x* (in the direction of the smaller horizontal dimension), *y* (in the direction of the larger horizontal dimension), and *z* (the vertical dimension), with a positive *x* pointing to technical east, a positive *y* to technical north, and a positive *z* axis directed upwards. These measurements lasted sixty minutes, with a time step of 0.01 second. From here, for one measurement we will have 360,000 samples (outputs). The results obtained from the measurements are accelerations versus time. For obtaining the natural frequencies, using fast Fourier transform (FFT) algorithm, these records are transformed into frequency domain (Kocaleva, 2021).

The first stage of the analysis of the obtained data is the detection of obvious errors from the measurements. An out of sync of the instruments may appear as an error. Although initially well synchronized, over time, due to loss of satellite signal, one of the instruments may show a different time than the other. However, these mistakes are not so common. More often, an error can appear in the measured signal if we have participation from the operation of a device in the house that causes forced vibrations, for example a washing machine. These forced vibrations contaminate the original signal with ambient excitations. The records for such and similar discrepancies will be analyzed at the beginning and the measurement for the location where the error was found will be repeated. Once we are satisfied that the records are cleared, we will proceed to process them (Manohar et al., 2012).

Due to the extremely "quiet" environment around the object on which the measurements were made, as well as the fact that the object has approximately the same dimensions in the three directions, in some measurements the peaks at the natural frequencies could not be observed. In those cases, the measurements at those stations were repeated. If measurements were made on objects in urban areas with pronounced ambient vibrations and on objects where the dimensions in the three directions differ substantially, the natural frequencies (eigenvalues) and their corresponding shape functions (eigenvectors) would be obtained easier and with fewer measurements.

Microtremors methodology

In this section we will examine velocity amplitudes. We do this to control the measurements obtained from the instruments. The longer the record is, the larger the amplitudes and closer to the ideal zero of oscillation we are. The goal of this section is to have approximately the same magnitude of positive and negative amplitudes in narrow band-pass recordings. We conduct the examination using the following methodology.

The first measured accelerations, i.e. the signal we get from the ambient vibration measurements, are not clean and they contain noise. On Figure 2 we show initially obtained record from the instrument and it looks like a curve that is far from the *x*-axis and the coordinate origin. This appearance is due to low frequency noise, and it pollutes the record. Our accelerometers measure acceleration in units of g = 9.81 m/s^2. During ambient vibration measurements, microtremors. Microtremors are defined as low-amplitude ambient vibrations caused by man-made or atmospheric disturbances. Observations of microtremors can provide useful information about the dynamical properties of the structure, such as period and mode shape.

For this purpose, to clean the records, first we filter the signal using a band pass filter with a wider range from 1 to 50 Hz. We choose the upper limit, considering that the Nyquist frequency for the selected time interval $\Delta t = 0.01$ s is $f_N = \frac{1}{2\Delta t} = 50$ Hz. By doing this we remove all frequencies lower than 1 and higher than 50 Hz, thus eliminating the low frequency (f < 1 Hz) noise of the instrument. The filtered record is shown in Figure 3. and we notice that now the signal oscillates around zero.

Acceleration, velocity, and displacement as physical quantities are related (Figure 4).

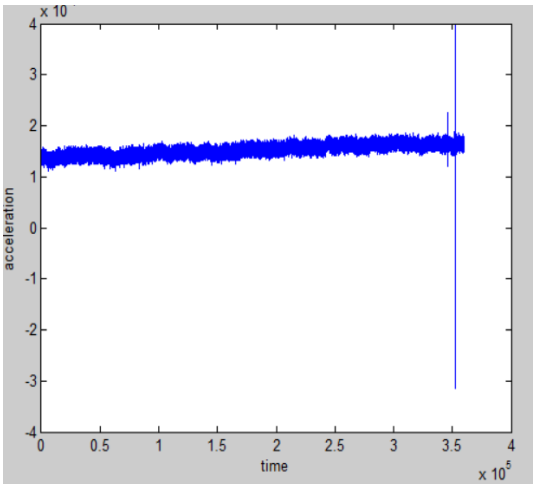

Fig. 2. Signal accelerations

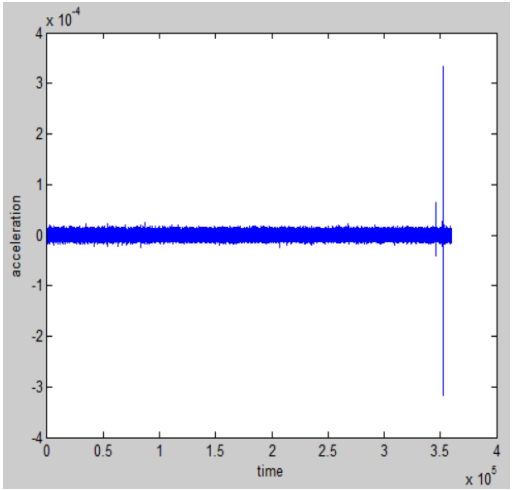

Fig. 3. Band-pass filtering on acceleration

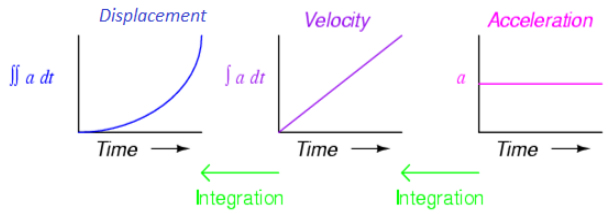

Fig. 4. Acceleration, velocity and displacement

Integrating the acceleration record, we get velocity record. Hence, the velocity will be expressed in units of $g \cdot s = 9.81$ m/s. We usually express the velocities of ambient vibrations in cm/s. To get it in cm/s, we first multiply the acceleration by a factor of 981. With that, we convert the acceleration from g to units of $\mathrm{cm/s^2}$.

Knowing that acceleration is the first derivative of velocity with time

$$a = \frac{dv}{dt}. \qquad (1),$$

Integrating (1), using central finite differences (CFD), for the velocity at the end of the time interval $[l \cdot \Delta t, (l+1) \cdot \Delta t]$ we get

$$v_{l+1} = v_l + a_{l+1/2} \cdot \Delta t, \qquad (2),$$

where $a_{l+1/2}$ is the acceleration in the middle of the considered interval. Since we have not obtained $a_{l+1/2}$ from the measurements, the standard procedure is to interpolate it linearly (mean value) from the two measurements at the beginning and end of the interval, i.e., $a_{l+1/2} \approx \frac{a_l + a_{l+1}}{2}$. By substituting this approximation in (2), for the velocity at the end of the considered interval we obtain

$$v_{l+1} = v_l + \left(\frac{a_l + a_{l+1}}{2}\right) \cdot \Delta t \qquad (3)$$

and it will be expressed in units of $\mathrm{cm/s}$.

It is known that when integrating, we get integration constants in the result. For this purpose, in principle, many initial or boundary conditions should be defined as there are integration constants in the solution. The equation (1) is a first-order differential equation in which solution one constant will appear. For this purpose, we must define the initial velocity (velocity at time t = 0 s) in equation (3).

For the initial speed we take $v_1 = 0$ (Figure 5). For an input of 360,000 accelerations, we get an output of 359,999 velocity values because the points v_l are midpoints of the accelerations.

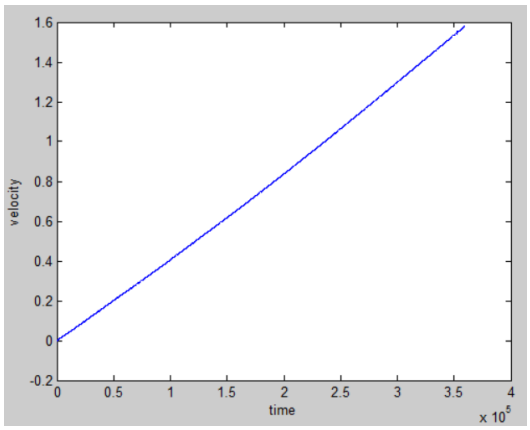

Fig. 5. Signal velocity

After finding the velocity, we need to filter it with a band-pass filter with a range of 1 to 50 Hz to eliminate distortions from the initial conditions and numerical noise (Figure 6).

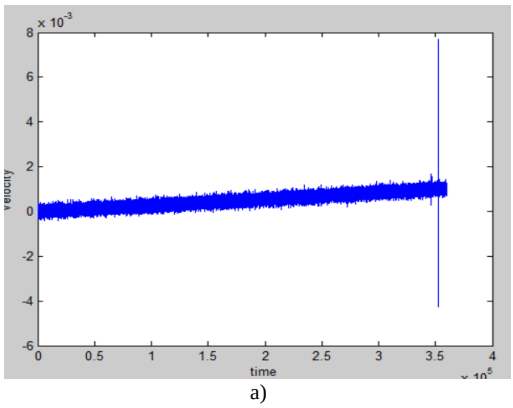

a)

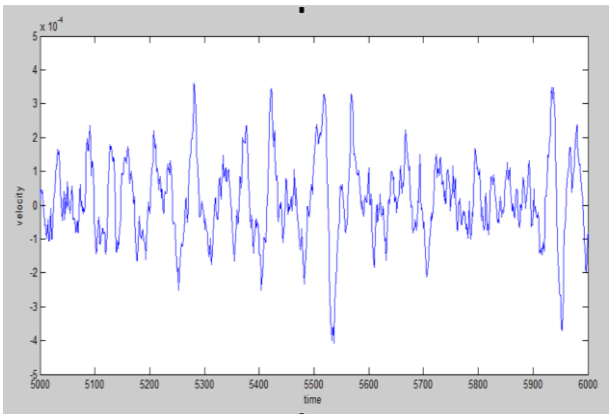

b

Fig. 6. Band-pass filtering on velocity. a) The hole signal; b) The part of signal (samples from 5000 to 6000)

This was filtering in a wider range. The next step is to obtain a narrower frequency, range centered around a fixed frequency in our case of 2, 4, 7, 10, 15 and 20 Hz using band-pass filtering. To obtain this frequency range, we use the Ormsby filter (Figures 7 and 8). The Ormsby filter is a pair filter $f(\omega) =$

$f(-\omega)$. This filter is a low-pass filter, which means that it filters out frequencies larger than previously defined cut-off frequency. The filter in the frequency domain has a trapezoidal shape (Figure 7) and is defined by two circular frequencies, a cut-off frequency, ω_c, and a termination frequency, ω_T. The filter completely rejects signal components with circular frequencies greater than ω_T, completely passes signal components with circular frequencies lower than ω_c, and partially passes signal components with circular frequencies between ω_c and ω_T.

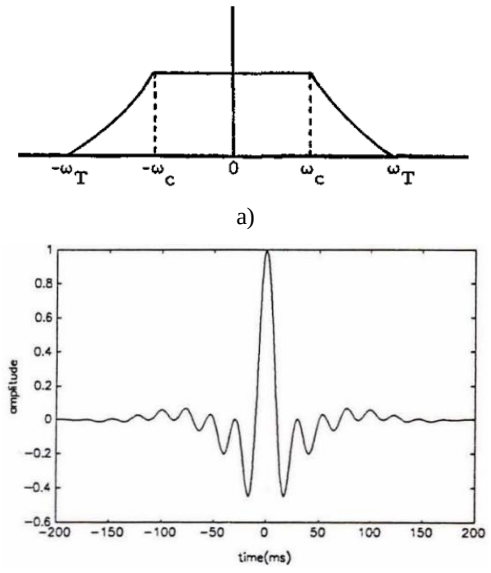

Fig. 7. Ormbsy filter. a) Ormbsy in frequency domain, b) Ormbsy in time domain

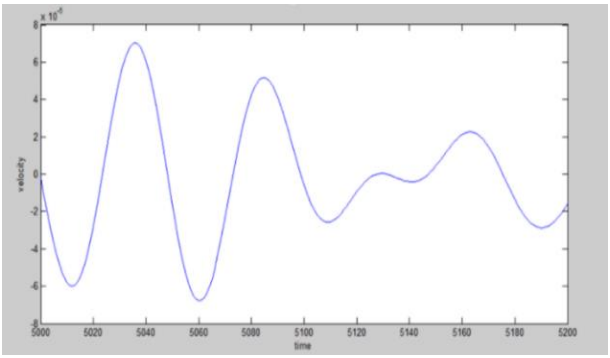

Fig. 8. Ormsby filter (2 Hz). a) The hole signal; b) The part of signal (samples from 5000 to 5200)

In practical applications, instead of circular frequencies ω_c and ω_T we use frequencies f_c and f_t which we get by dividing ω_c and ω_T by $2 \cdot \pi$. We can also denote these frequencies as the termination frequency by f_t and the cutoff frequency by f_c. Following Ormsby (1961) the constant λ_r can be defined as

$$\lambda_r = \frac{|f_t - f_c|}{f_s}, \qquad (4)$$

where $f_s = \frac{1}{\Delta t}$ is the sampling frequency and for $\Delta t = 0.01\ s$, $f_s = 100$ Hz. The number of filter weights N is $N = \frac{1}{\lambda_r}$ (Trifunac, 1971) and from here it follows that $\lambda_r \cdot N = 1$. The higher the sampling frequency f_s, the smaller the filter ramp λ_r is, and the larger the number of weights N. N and λ_r are inversely proportional.

Calculation and representation of microtremors

To quantify microtremors as excitations coming into the building from the ground through the foundation, we proceed as follows:

1) We filter the measured acceleration in the reference point (Slave) in a wide frequency range 1 – 50 Hz, and for sampling frequency $f_s = 100$ Hz and continuous measurement of 60 minutes we get 360 000 accelerations.

2) We integrate the filtered record from the previous point (1) with the equation (3) whereby we get the velocities in 359 999 points.

3) We filter the velocities obtained in 2) to eliminate distortions from initial conditions and numerical noises with the same frequency range (1 – 50 Hz).

4) We filter the filtered records from 3) again with a narrower frequency range centered around several fixed frequencies f_{0i} = (2, 4, 7, 10, 15, 20 Hz).

5) We calculate the differences between the neighboring maximum and minimum amplitudes (peak-to-peak), for the entire velocity record (Figure 14).

6) We calculate the mean differences of the peak-to-peak amplitudes.

7) We divide the mean difference from 6) by the central fixed frequency. We save this result.

8) We return to step 4) and repeat the procedure for all central fixed frequencies.

a) Center frequency in 2 Hz with $f_t = 1.5$ Hz, $f_c = 1.75$ Hz on the left and $f_c = 2.25$ Hz, $f_t = 2.5$ Hz on the right.

$$\lambda_r = \frac{|1.5-1.75|}{100} = \frac{|2.5-2.25|}{100} = \frac{0.25}{100} = 0.0025,$$

$$N = \frac{1}{0.0025} = 400.$$

b) Center frequency in 4 Hz with $f_t = 3.0$ Hz, $f_c = 3.5$ Hz on the left and $f_c = 4.5$ Hz, $f_t = 5.0$ Hz on the right (Figure 9).

$$\lambda_r = \frac{|3.0-3.5|}{100} = \frac{|5.0-4.5|}{100} = \frac{0.5}{100} = 0.005,$$

$$N = \frac{1}{0.005} = 200.$$

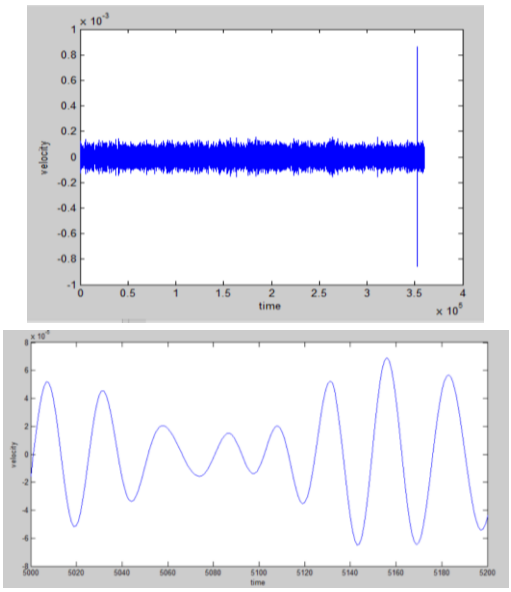

Fig. 9. Ormsby filter (4 Hz). a) The hole signal; b) The part of signal (samples from 5000 to 5200)

c) Center frequency in 7 Hz with $f_t = 6.0$ Hz, $f_c = 6.5$ Hz on the left and $f_c = 7.5$ Hz, $f_t = 8.0$ Hz on the right (Figure 10).

$$\lambda_r = \frac{|9.0-9.5|}{100} = \frac{|11.0-10.5|}{100} = \frac{0.5}{100} = 0.005,$$
$$N = \frac{1}{0.005} = 200.$$

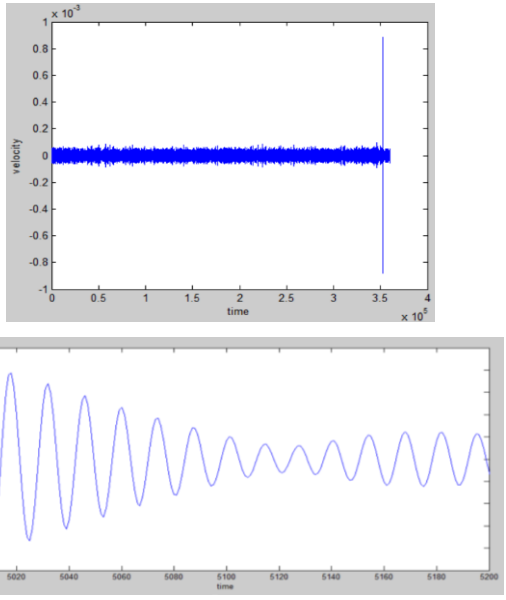

Fig. 10. Ormsby filter (7 Hz). a) The hole signal; b) The part of signal (samples from 5000 to 5200)

d) Center frequency in 10 Hz with $f_t = 9.0$ Hz, $f_c = 9.5$ Hz on the left and $f_c = 10.5$ Hz, $f_t = 11.0$ Hz on the right (Figure 11).

$$\lambda_r = \frac{|9.0-9.5|}{100} = \frac{|11.0-10.5|}{100} = \frac{0.5}{100} = 0.005$$
$$N = \frac{1}{0.005} = 200.$$

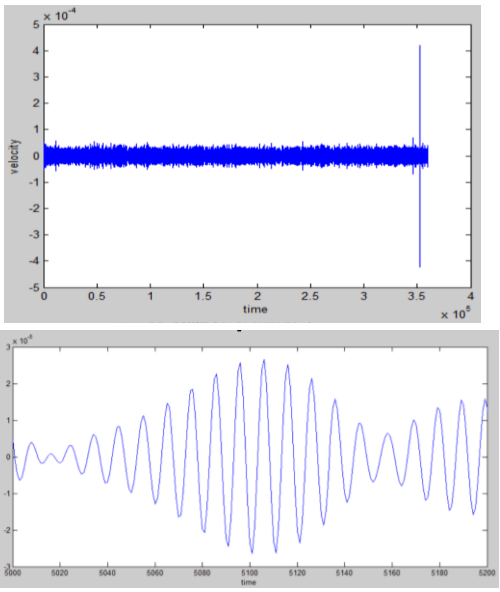

Fig. 11. Ormsby filter (10 Hz). a) The hole signal; b) The part of signal (samples from 5000 to 5200)

e) Center frequency in 15 Hz with $f_t = 13.5$ Hz, $f_c = 14.7$ Hz on the left and $f_c = 15.7$ Hz, $f_t = 16.5$ Hz on the right (Figure 12).

$$\lambda_r = \frac{|13.5-14.7|}{100} = \frac{|16.5-15.7|}{100} = \frac{0.8}{100} = 0.008$$
$$N = \frac{1}{0.008} = 125.$$

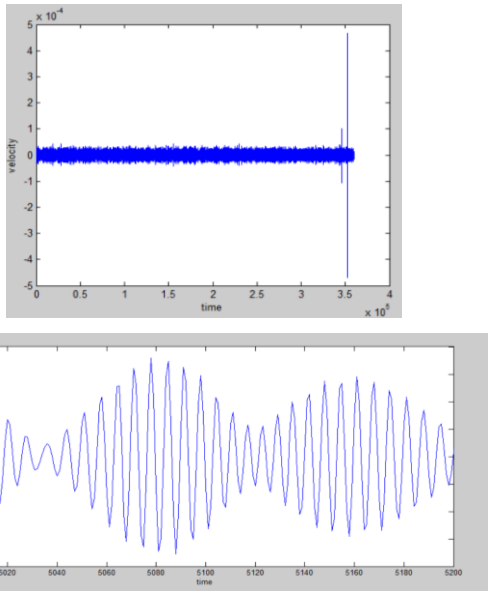

Fig. 12. Ormsby filter (15 Hz). a) The hole signal; b) The part of signal (samples from 5000 to 5200)

f) Center frequency in 20 Hz with $f_t = 18.0$ Hz, $f_c = 19.0\ Hz$ on the left and $f_c = 21.0$ Hz, $f_t = 22.0$ Hz on the right (Figure 13).

$$\lambda_r = \frac{|18.0-19.0|}{100} = \frac{|22.0-21.0|}{100} = \frac{1}{100} = 0.01$$
$$N = \frac{1}{0.01} = 100.$$

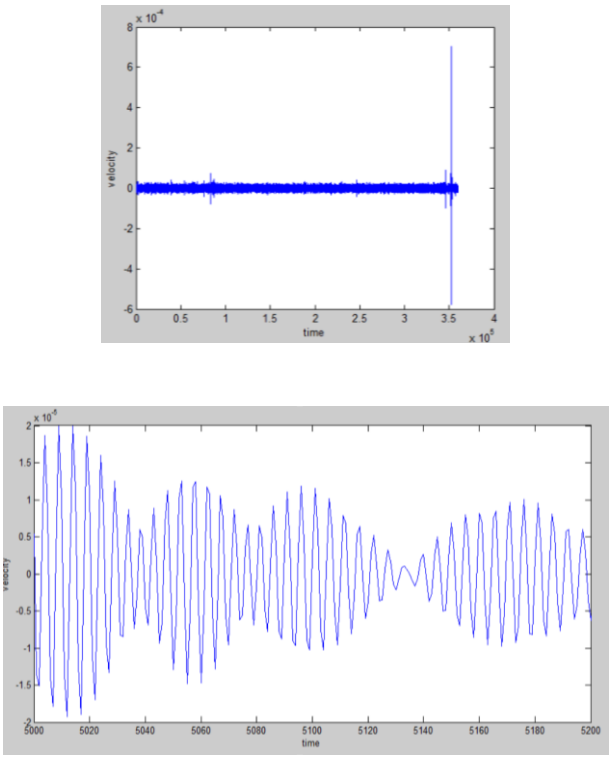

Fig. 13. Ormsby filter (20 Hz), a) The hole signal; b) The part of signal (samples from 5000 to 5200)

After filtering we find the difference between the maximum and minimum amplitudes (peak to peak amplitude) for the entire length of the signal.

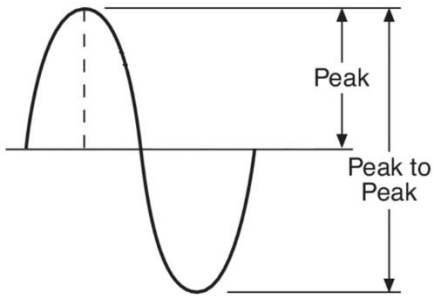

Fig. 14. Peak-to-peak amplitude

Going through the velocity record, we find the amplitudes by considering three adjacent points a_l, a_{l+1}, a_{l+2} that meet the condition $(a_{l+1} - a_l) \cdot (a_{l+2} - a_{l+1}) < 0$. Positive amplitudes A_p are those where $a_l < a_{l+1}$ and $a_{l+1} > a_{l+2}$, and negative A_n are $a_l > a_{l+1}$ and $a_{l+1} < a_{l+2}$. Also, here we check if two successive amplitudes are with the same sign, positive or negative, and if we have such a case, we ignore the first amplitude and continue with the next one.

The difference between the maximum and minimum amplitudes (peak-to-peak amplitude) is found with the formula

$$\mathrm{dif}f1 = A_p(a_{l+1}) - A_n(a_{l+1})$$

for each pair of positive and negative amplitude. We find the average value

$$\mathrm{average} = \frac{\sum \mathrm{dif}f1}{D},$$

where D is the total number of pairs of positive and negative amplitude. Average shows the deviation about the zero axis or the rate of oscillation about an axis that does not coincide with the ideal axis. This value represents the ideal axis when all amplitudes would be the same.

Then we divide the mean value by the center frequency

$$f_{\mathrm{result}} = \frac{\mathrm{average}}{f}.$$

The represented signal with a frequency of 2 Hz has a total of 14 361 amplitudes, or 7181 positive and 7180 negative amplitudes. The final value of the peak-to-peak amplitude is:

$$f_{\mathrm{result}} = \frac{\mathrm{average}}{2} = 7.921937 \cdot 10^{-5}.$$

A signal with a frequency of 4 Hz has 28726 amplitudes. Same number of positive and negative amplitudes (14363 each). The result is:

$$f_{\mathrm{result}} = \frac{\mathrm{average}}{4} = 2.356210280 \cdot 10^{-5}.$$

A signal with a frequency of 7 Hz has 25189 even and 25188 odd amplitudes.

$$f_{\mathrm{result}} = \frac{\mathrm{average}}{7} = 6.92503818 \cdot 10^{-6}.$$

This same signal with a frequency of 10 Hz has 35988 positive and the same number of negative amplitudes. For a frequency of 10 Hz the result is:

$$f_{\mathrm{result}} = \frac{\mathrm{average}}{10} = 3.13064129 \cdot 10^{-6}.$$

For 15 Hz, this signal has 53966 positive and as many negative amplitudes. The result for this frequency is:

$$f_{\mathrm{result}} = \frac{\mathrm{average}}{15} = 1.56613589 \cdot 10^{-6}.$$

And finally, with a frequency of 20 Hz the signal has 143 926 amplitudes. 71963 are positive and 71963 are negative. The peak-to-peak amplitude value is:

$$f_{\mathrm{result}} = \frac{\mathrm{average}}{20} = 9.3155847 \cdot 10^{-7}.$$

We save the obtained results (f_{result}) and plot them on a graph. We repeat the whole procedure for

2 different records, one of which represents the *y* component, and the other the *z* component obtained from the Slave instrument. We draw the graph using a decimal and logarithmic scale. We use the logarithmic scale for a better insight into the ordinates at higher frequencies (f >10 Hz).

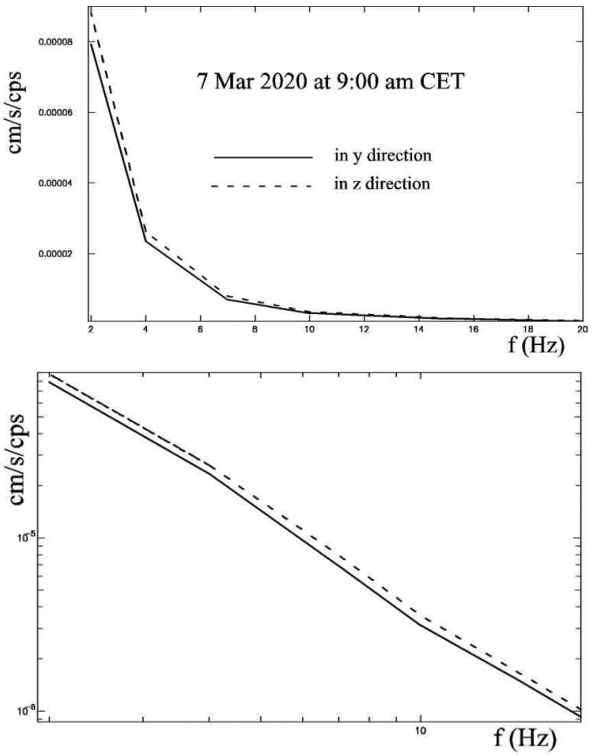

Fig. 15. Microtremors (velocity per frequency) in the Berovo house in decimal (above) and in logarithmic (below) scale

From the above figures it can be concluded that the velocities decrease with increasing frequency and for horizontal velocities they decrease from $8 \cdot 10^{-5}$ to $9 \cdot 10^{-7}$ cm/s/Hz, and for vertical velocities (dashed lines) from $9 \cdot 10^{-5}$ to 10^{-6} cm/s/Hz. Figure 16 shows the peak-to-peak amplitudes of velocities in three orthogonal instrument directions induced by microtremors in rural environment in Pennsylvania, USA. To compare the results with our measurements, we observed the velocities in the frequency range from 2 to 20 hertz. It can be noted that in this frequency range the velocities do not show large variations in relation to the frequencies and range from 10^{-5} to $8 \cdot 10^{-5}$ cm/s/Hz for the horizontal direction and from $1.5 \cdot 10^{-6}$ to 10^{-5} cm/s/Hz for vertical direction. If we make a comparison, we can conclude that the values of the velocities, especially those in the horizontal direction, are similar.

For a comparison of microtremors at the location of house on Berovo Lake and microtremors at locations in rural areas of the United States, we show in Figure 17 the mean differences in peak-to-peak vertical velocities normalized by the center frequency in Hz (cps) or the so-called "P to P" velocities. From Figure 17 it can be noticed that at frequency range from 2 to 20 Hz, the velocity decreases with increasing frequency.

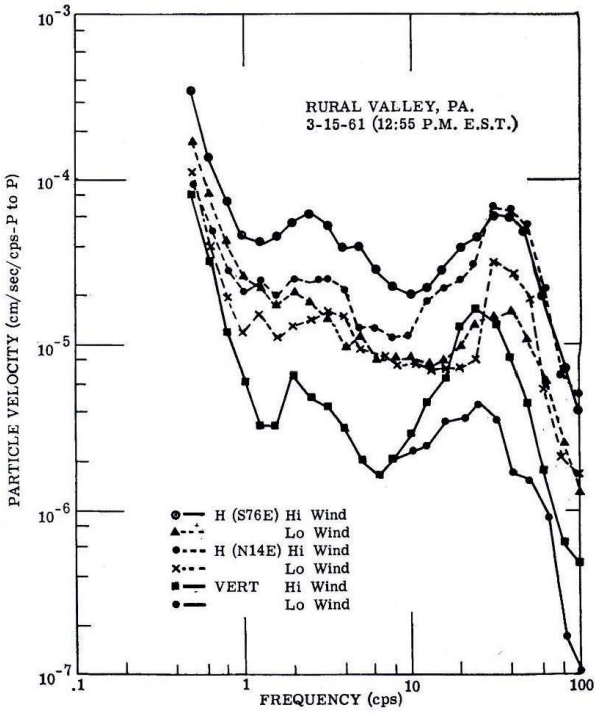

Fig. 16. Microtremor apmlitudes in rural valley, Pennsylvania

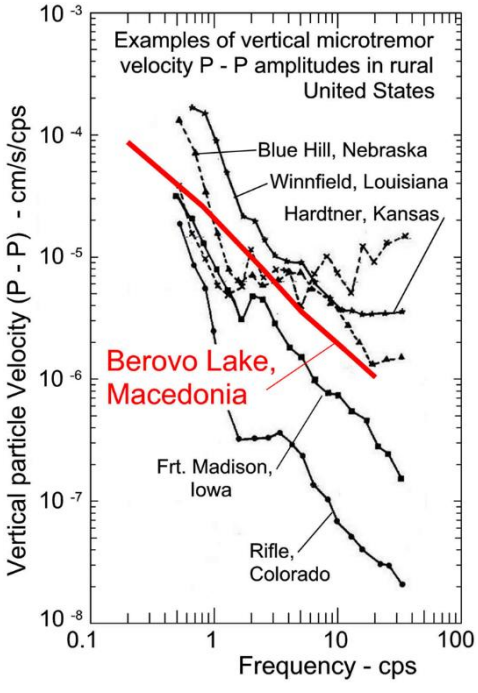

Fig. 17. Microtremor in Berovo vs in rural United States

CONCLUSION AND SUMMARY

Using sensitive instruments, by means of numerial methods, mathematical transformations, and software for digital processing, based on measured small, ambient vibrations, we can find the natural characteristics of the building. Ambient vibration measurements should be carried out at a dense set of points, thus providing detailed information about the spatial properties of the object. In tall objects, where one dimension (height) is much larger than the other two (width and length), measurements at fewer points, through the analysis of the transfer function of the system or through the power spectral density (PSD) are sufficient to determine the first few natural frequencies and their corresponding modal shapes. For three-dimensional objects with irregular geometry, especially for objects with approximately the same dimensions in three mutually orthogonal directions, measurements at many locations are necessary and it is recommended to use two instruments (transfer functions) instead of one instrument (PSD method). This recommendation is since the measurements at two different locations of the building happen at different times when the external excitations may change. Using two instruments, one at fixed reference position (Slave), usually at point with low motion, and one at the considered location (Master), dividing the Fourier spectrum of the Master with the Fourier spectrum of the Slave one can find the transfer function, $TF(f) = \frac{M(f)}{S(f)}$. The role of the Slave is to normalize the spectrum of the Master and with that to eliminate the variation of the external conditions occurring during the measurements at different points of the structure. Moreover, because the motion at the Slave is lower than the one at the Master, this division increases the Fourier amplitudes, and the peaks of the transfer functions are more pronounced. Finally, ambient vibration tests are "complete", "full scale" experiments. Even carefully planned laboratory experiments will represent only those aspects of the problem that the experiment designer chose to study and includes in the model. The best and most complete laboratory tests can verify and measure only those aspects of the problem that the researcher knows. Full ambient vibration tests present a completely different situation that cannot be easily controlled. The built environment contains all the properties of reality. We just must find wise ways to discover, record and interpret this reality. That is why the processing of ambient vibrations and based on them the determination of natural frequencies and modal forms is on the border between science and art.

REFERENCES

Abdel-Ghaffar, A. M., Scanlan, R. H., Diehl, J. (1984): Full-scale ambient vibration measurements of the Golden Gate suspension bridge. In: *Proceedings of the Eighth World Conference on Earthquake Engineering*, Vol. 6, *Prentice-Hall, Inc., Englewood Cliffs, New Jersey*, pp. 881–888).

Abdel-Ghaffar, A. M., Housner, G. W. (1977): *An analysis of the dynamic characteristics of a suspension bridge by ambient vibration measurements* (No. EERL-77-01). California Institute of Technology.

Abdel-Ghaffar, A. M., Housner, G. W. (1978): Ambient vibration tests of suspension bridge. *Journal of the Engineering Mechanics Division*, **104** (5), 983–999.

Abdel-Ghaffar, A. M., Scott, R. F. (1981): Vibration tests of full-scale earth dam. *Journal of the Geotechnical Engineering Division*, **107** (3), 241–269.

Brownjohn, J. M. (2003): Ambient vibration studies for system identification of tall buildings. *Earthquake Engineering & Structural Dynamics*, **32** (1), 71–95.

Brownjohn, J. M. (2007): Structural health monitoring of civil infrastructure. *Philosophical Transactions of the Royal Society. A: Mathematical, Physical and Engineering Sciences*, **365** (1851), 589–622.

Carder, D. S. (1936): Vibration observations, Chapter 5 in *Earthquake Investigations in California 1934–1935*, Special Publication No. 201, Coast and Geologic Survey, U.S. Dept. of Commerce, Washington, D.C.

Gičev, V., Trifunac, M. D., Todorovska, M. I., Kocaleva, M., Stojanova, A., Kokalanov, V. (2021): Ambient vibration measurements in an irregular building. *Soil Dynamics and Earthquake Engineering*, Volume **141**, pp. 1–22. ISSN 0267-7261. https://doi.org/10.1016/j.soildyn.2020.106484

CS Instruments, (2019): Eqresponder: New generation plug-and-play accelerometer from CSITechnical Manual.

Kapsarov, H., Miliččvić, M. (1986): Comparison between experimental and theoretical investigations of high RC chimneys for mathematical formulation. In: *8th European Conference On Earthquake Engineering (8ECEE), Lisbon* Vol. **4**, pp. 73–80.

Klasky, P. S., Staton, R. R., Stubbs, I. R., Fix, J. E. (1973): Structural Monitoring Techniques And Instrumentation For Nuclear Power Plants. In: *Proc. Fifth World Conference on Earthquake Engineering*, International Assn. for Earthquake Engineering, Rome, pp. 1077–1080.

Ko, J. M., Bao, Z. W. (Eds.) (1985): *Ambient Vibration Measurements on Existing Tall Buildings in Hong Kong*. Civil & Structural Engineering Department, Hong Kong Polytechnic.

Kocaleva, M. (2021): *Natural periods of civil engineering objects obtained by measuring and processing of ambient vibrations tests*. PhD thesis, Faculty of Computer Science, Universiry Goce Delčev – Štip.

Kokalanov, V., Trifunac, M., Gicev, V., Kocaleva, M., Stojanova, A. (2022): High frequency calibration of a finite element model of an irregular building via ambient vibration measurements. *Soil Dynamics and Earthquake Engineering*, Volume **153**. ISSN 0267-7261. https://doi.org/10.1016/j.soildyn.2021.107005

Luco, J. E., Trifunac, M. D., Udwadia, F. E. (1975): An experimental study of ground deformations caused by soil-structure interaction. In: *Proc. US National Conf. on Earthquake Eng.*, pp. 136–145.

Luz, E., Gurr-Beyer, C., Stoecklin, W. (1983). Identification of natural frequencies and modes of a nuclear power plant by means of excitation with environment noise. *Transactions of the 7th International Conference on Structural Mechanics in Reactor Technology*, North Holland Physics Publishing, Arnsterdam, Vol. K(b): 437–443.

Manohar, A. K., Sengupta, K., G, T., Gogoi, I., (2012): Earthquake vulnerability assessment of buildings in Guwahati. *International Journal of Earth Sciences and Engineering*, **5** (3), pp. 618–623.

Moslem K, Trifunac M. D. (1986): *Effects of soil structure inteaction on the response of buildings during strong earthquake ground motions*, Report No. 86 04, Dept. of Civil Eng., Univ. of Southern California, Los Angeles, California.

Mulhern, M. R., Maley, R. P. (1973): Building period measurements before, during and after the San Fernando, California, earthquake of February 9, 1971, U.S. Depart. of Commerce, National Oceanic and Atmospheric Administration, Washington D.C., Vol. **I**, Part B: 725–733.

Ormsby, J. F. A, (1961): Design of numerical filters with application to missile data processing. Assoc. *Computing Machinery Journal*, **8**, 440–466.

Rahmani, M., Todorovska, M. I. (2014): 1D system identifycation of a 54-story steel frame building by seismic interferometry. *Earthquake Engineering and Structural Dynamics*. https://doi.org/10.1002/eqe.2364.

Rodriguez-Cuevas, N. (1989): Structural evaluation of buildings in Mexico City, Lessons learned from the 1985 Mexico Earthquake, Report 89 02, Earthquake Engineering Research Inst., El Cerrito, California, 198–199.

Sawada, S. (2004): A simplified equation to approximate natural period of layered ground on the elastic bedrock. *13th World Conference on Earthquake Engineering*, 1100.

Taskov L, Krstevska L (1998). Ambient vibration measurements of a R/C silo for grain storage in Skopje, *Proc. Eleventh Europ. Conf. Earthq. Eng*. [computer file], A. A. Balkema, Rotterdam.

Trifunac M. D (1970): *Ambient vibration Test of a 39-story steel frame building*, Report EERL 70–02, Earthquake Engineering Research Laboratory, California Institute of Technology, Pasadena, California.

Trifunac, M. D. (1971): Zero baseline correction of strong motion accelerograms. *Bulletin Seism. Soc. of America*, vol. **61**, 5, 1201–1211.

Trifunac, M. D., Ivanović, S. S., Todorovska, M. I. (1999): *Seven story reinforced concrete building in Van Nuys, California: strong motion data recorded between 7 Feb. 1971 and 9 Dec. 1994, and description of demage following Northridge 17 Jan. 1994 earthquake*. Report CE 99-02.

Trifunac, M. D., Ivanović, S. S., Todorovska, M. I. (2001a): Apparent periods of a building. I: Fourier analysis. *Journal of Structural Engineering*. https://doi.org/10.1061/(ASCE)0733-9445(2001)127:5(517)

Trifunac, M. D., Ivanović, S. S., Todorovska, M. I. (2001b): Apparent periods of a building. II: Time-frequency analysis. *Journal of Structural Engineerin*g. https://doi.org/10.1061/(ASCE)0733-9445(2001)127:5(527)

Wong, H. L., Luco, J. E., Trifunac, M. D. (1977): Contact stresses and ground motion generated by soil-structure interaction. *Earthquake Engineering Structural Dynamics*, **5** (1), 67–79.

Р е з и м е

АНАЛИЗА НА МИКРОТРЕМОРИ СО МЕРЕЊЕ И ПРОЦЕСИРАЊЕ НА ТЕСТОВИ ЗА АМБИЕНТАЛНИ ВИБРАЦИИ

Мирјана Коцалева Витанова, Владо Гичев

Факултет за информатика, Универзитет „Гоце Делчев“
бул. Крсте Мисирков 10А, Штип, Република Северна Македонија
mirjana.kocaleva@ugd.edu.mk

Клучни зборови: природни катастрофи; микротремори; амплитуди од врв до врв

Микротреморите, вибрации на почвата од мал обем, обично со амплитуди во опсег од микрометри до милиметри, се покажаа како вредна алатка за проучување на различни аспекти на подземните својства и динамика на Земјата. Овој труд нуди преглед на методологиите кои се користат за откривање, анализа и интерпретација на микротреморите применети за двокатна армирано-бетонска зграда во Берово.